energies

MDPI

Article

A Hybrid Energy System Based on Externally Fired Micro Gas Turbines, Waste Heat Recovery and Gasification Systems: An Energetic and Exergetic Performance Analysis

Fabrizio Reale * and Patrizio Massoli

Institute of Sciences and Technologies for Sustainable Energy and Mobility (STEMS), National Research Council, 80125 Napoli, Italy; patrizio.massoli@stems.cnr.it
* Correspondence: fabrizio.reale@cnr.it

Abstract: The opportunities related to the adoption of synthetic gaseous fuels derived from solid biomass are limited by the issues caused by the peculiarities of the syngas. The aim of this paper is to analyze several possible layouts of hybrid energy systems, in which the main thermal source is the organic fraction of municipal solid wastes. The case of a small community of about 1000 persons is analyzed in this paper. The examined layouts coupled an externally fired micro gas turbine with a waste heat recovery system based on both an Organic Rankine Cycle and supercritical CO_2 gas turbines. A thermodynamic analysis has been carried out through the use of the commercial software Thermoflex 31, considering the losses of each component and the non-ideal behavior of the fluids. The results of the numerical analysis highlight that the introduction of a waste heat recovery system leads to an increase of at least 16% in the available net power, while a cascade hybrid energy grid can lead to a power enhancement of about 29%, with a considerable increase also in the energetic and exergetic global efficiencies.

Keywords: waste heat recovery; sCO_2 gas turbine; externally fired micro gas turbine; integrated energy system

Citation: Reale, F.; Massoli, P. A Hybrid Energy System Based on Externally Fired Micro Gas Turbines, Waste Heat Recovery and Gasification Systems: An Energetic and Exergetic Performance Analysis. *Energies* **2024**, *17*, 3621. https://doi.org/10.3390/en17153621

Academic Editor: George Kosmadakis

Received: 1 July 2024
Revised: 17 July 2024
Accepted: 19 July 2024
Published: 24 July 2024

1. Introduction

Biomass is a renewable source which can contribute to diversifying energetic sources, reducing the dependency on fossil fuels, and also controlling greenhouse emissions [1].

In the early years of the XXI s., the research community's interest in the use of biomass as an energy source grew, and in recent years, it has increased again [2]. While energy-dedicated crops involve several ethical issues, byproducts of the agricultural industries or pruning and, more generally, organic waste residuals allow us to overcome these issues and to consider biomass a valid energy source [1,3]. Based on the International Energy Agency's considerations, the world is using just a minimal fraction of the potential to produce gas from organic waste, while this could cover around 20% of the current global demand for gas [4].

Biomass gasification can reduce the issues related to its direct combustion, since the combustion of syngas results in cleaner and more efficient gas production, even if it provides other issues related to the cost and efficiency of the process. In addition, a critical aspect is the difficulty of achieving satisfactory compatibility between syngas and the conversion systems based on engines [5].

In this context, externally fired (or indirect fired) gas turbines (EFGTs) can represent a suitable solution to operate with biomass as fuel, since the thermal source heats the working fluid through a heat exchanger and, consequently, the combustion products do not directly participate in the thermodynamic cycle. Thus, the requirements related to fuel cleaning and composition can be lowered [6].

EFGTs can burn solid fuels or critical liquid or gaseous fuels whose use in gas turbines involves several issues because the problems related to exhaust composition are shifted from gas turbine components to the heat exchanger, which assumes a fundamental role. It has to ensure an efficient heat exchange at high temperature in order to guarantee a satisfactory turbine inlet temperature, even in the presence of an aggressive working fluid rich in particulates [7,8]. However, at the same time, the opportunities related to gasification in small-scale power plants have been analyzed in the literature for both internally and externally fired gas turbines [9,10].

Several layouts based on externally fired micro gas turbines (EFMGTs) have been studied in the literature through the adoption of various numerical approaches, as shown in [11,12].

Traverso et al. analyzed the use of EFMGTs in the case of the combustion of solid biomass. In their proposed layout, the traditional internal combustor of a regenerative micro gas turbine (MGT) is replaced by a heat exchanger and an external combustion chamber, located at the exit of the turbine [13]. In the dual-fuel configuration, both internal combustion and external furnace/combustion chambers coexist, as proposed by Pantaleo et al. [14] and Riccio and Chiaramonti [15]. In these cases, fresh air is first heated by the high-temperature exhausts of the biomass burned in a furnace, and then, it participates in combustion in a traditional combustor. These layouts allow for the flexible use of both solid and gaseous fuels.

A limit of the externally fired gas turbine is the low efficiency but the high temperature of the exhausts allows us to consider waste heat recovery (WHR) a viable solution to increase the performance and overall efficiency of the hybrid energy system.

The subcritical Organic Rankine Cycle (ORC) is the reference technology for converting waste heat to electricity [16]. In particular, based on the temperature levels typical of the exhaust gases (the heat source), an Organic Rankine Cycle (ORC) is often considered the bottoming cycle to be coupled with micro gas turbines [17–19]. The integration of an MGT with a bottoming ORC allows us to increase the combined cycle efficiency by up to 15% [20].

Regarding the adoption of biomass-derived fuels in MGT-ORC layouts, in a previous article, the authors proposed an integrated energy system based on MGT, ORC and a gasifier in which the fuel was a mix of the syngas and biogas obtained via gasification and anaerobic digestion, respectively. The results of both thermodynamic and CFD simulations highlighted that syngas/biogas blends can contribute to increasing the allowability of these fuels in an energy system designed for natural gas and also to extending the limits related to their adoption, without any redesign of the combustion chamber and/or fuel feeding system [21].

EFMGTs integrated with waste heat recovery systems can be a solution to overcome both the issues related to the use of biofuels in micro gas turbines and the low efficiency typical of EFMGTs. The integration of ORC systems with EFMGTs can lead to a further, different critical issue: the temperature levels of the heat source. In fact, ORC systems are a valid technical solution for waste heat recovery when the heat source temperature is between 100 °C and 400 °C and the upper limit is imposed by the flammability, low chemical stability and risk of decomposition of the organic fluids at high temperature [22,23].

For higher heat source temperature levels, supercritical carbon dioxide (sCO_2) closed Brayton cycles can be considered a solution, also taking in account that some of the most suitable organic fluids in terms of global warming potential (GWP) and ozone depletion potential (ODP) perform better at medium–low temperature levels. The peculiarities of CO_2 in transcritical and supercritical conditions allow for its use also in cases of heat pumps for domestic hot water or room heating [24].

The sCO_2 Brayton cycle presents many advantages with respect to conventional steam Rankine cycles or Brayton cycles due to its simplicity, compactness and higher efficiency, and it is actually considered a valid solution in nuclear, geothermal, solar thermal and

waste heat recovery applications. Several layout schemes are considered to obtain the best performance levels: recompression, regenerative, intercooled and so on [25,26].

Furthermore, the sCO_2 closed Brayton cycle allows for further cascade waste heat recovery, through the integration of sCO_2 gas turbines and ORC, to recuperate the residual thermal power and to further increase the overall power [27].

Regarding any economic evaluation, it is important to consider that the market of EFMGTs is currently very limited and that the sCO_2 gas turbine is a novel technology. Nevertheless, various studies can help us to better define this point. The utilization of biomass-derived fuels in EFGTs is economically sustainable when biomass is available as a product or byproduct in abundance without transport costs [6]. However, the collaboration between gasification and an internal combustion engine appears to be less expensive with respect to EFGT systems, although increasing interest in this technology can lead to a reduction in costs [6,28]. The heat exchanger represents one of the most expensive components and the cost increases with the maximum temperature allowed [6,29].

Ancona et al. [30] compared bottoming cycles based on sCO_2 GTs and the ORC, analyzing the investment costs, starting from given correlations and references [31,32]. They concluded that the plant investment cost is higher in the case of sCO_2 GTs compared to the use of an ORC. This is primarily due to the cost of sCO_2 heat exchangers.

The aim of this paper is to identify a small-scale hybrid energy system able to use the organic fraction of municipal solid waste as fuel with satisfactory performance levels. To this end, several hybrid energy systems based on an externally fired micro gas turbine with a dual-fuel option have been examined and compared, considering both traditional fossil fuel (i.e., natural gas) and syngas. The quantity and composition of syngas are derived from [33], with the understanding that the solid biomass flow is limited to approximately 100 kg/h, a value estimated based on the waste production of a community of approximately 1000 individuals.

The externally fired solution allows us to overcome the constraints related to the use of syngas, as highlighted in [21], also considering the presence of impurities that may damage the turbine blades. The lower overall efficiency, which is typical of externally fired gas turbines, can be enhanced through the utilization of the dual-fuel option and the waste heat recovery system.

From this perspective, the higher temperatures of the exhausts are useful to increase the quality of the wasted heat. Nine different configurations have been analyzed in terms of energetic and exergetic performance indices: the dual-fuel EFMGT and eight integrated layouts with an ORC and/or sCO_2 gas turbines. A comparative analysis allows for the identification of the positive effects of integrating these energy systems into a novel one. This analysis helps us to determine the optimal layout in terms of energetic and exergetic efficiency and net power, also considering the number of components and heat exchangers.

2. Hybrid Energy System Layout

The aim of this study is to examine different hybrid energy systems based on an externally fired micro gas turbine derived from a commercial MGT, model Turbec T100 (currently manufactured by Ansaldo Energia (Genoa, Italy) as AE T100), which is a regenerative single-shaft plant able to achieve an overall efficiency close to 30% at full load and in design ambient conditions [27].

The proposed EFMGT follows a dual-fuel scheme already shown in the literature [9,10] and is shown in Figure 1 (layout 0). The gasification system is not depicted for the sake of simplicity. The introduction of the dual-fuel strategy allows us to increase both the overall energetic efficiency and fuel flexibility. Indeed, the proposed layout can operate in three different modes: pure natural gas, pure biomass, and dual-fuel mode. The use of a traditional fuel, i.e., methane, permits us to compensate for any variation in the availability or composition, and consequently, the lower heating value, of biomass. In this way, the

nominal load can be guaranteed in cases of a scarcity of biomass. It is clear that as the percentage of methane increases, the electrical efficiency also rises.

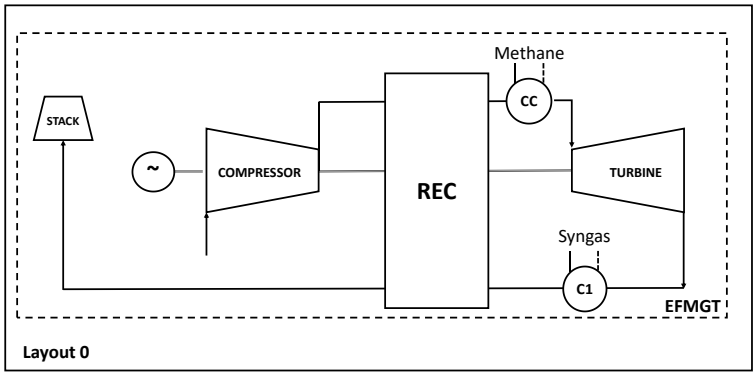

Figure 1. Layout 0: dual-fuel externally fired micro gas turbine (EFMGT).

The first two waste heat recovery (WHR) bottoming systems are a recuperated Organic Rankine Cycle (ORC) (layout 1) and a simple sCO_2 closed Brayton cycle (SCBC) (layout 2), both represented in Figure 2. In all layouts which will be depicted, air/gas flows are represented by black lines, while sCO_2 and the organic fluid are reported in red and orange, respectively.

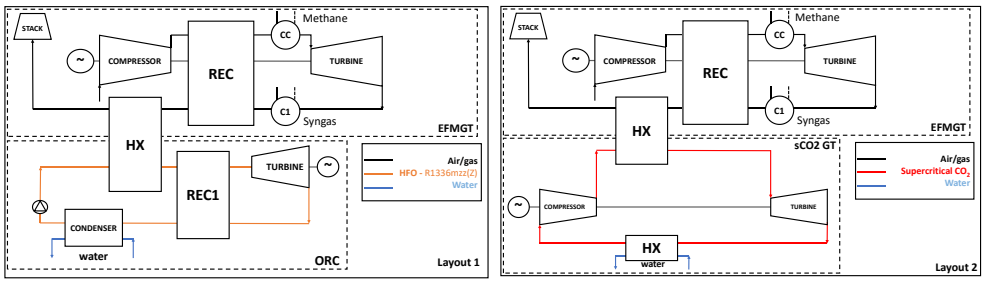

Figure 2. EFMGT plus ORC (**left**, layout 1) and EFMGT plus simple CO_2 GT (**right**, layout 2).

In these schemes, the thermal power available at the exhausts of the EFMGT represents the input of a waste heat recovery system. Layout 1 is derived from the MGT-ORC–gasifier hybrid system proposed in [21].

The further layouts present an increasing complexity of WHR with respect to the simple Brayton cycle (layout 1), where heat exchangers, valves or turbines are added.

Figure 3 shows the schemes with a recuperated SCBC (layout 3) and a preheated and recuperated supercritical CO_2 gas turbine (sCO_2 GT) (layout 4), while layout 5 is a partially preheated and recuperated sCO_2 GT (Figure 4, left). The latter cases (layouts 6, 7 and 8) combine an sCO_2 GT and ORC in a cascade cycle: the sCO_2 GT receives heat from the topping EFMGT, and in turn, it gives off heat to the latter energy system. The ORC system is a simple one, without any further internal heat exchanger, as shown in Figure 2, due to the need to keep the temperature at the sCO_2 compressor inlet higher than the critical temperature but as close as possible to that value. The three cascade layouts differ among them as regards the middle cycle: the first is a simple sCO_2 gas turbine (layout 6, Figure 4), while the others are a recuperated one (layout 7) and a preheated and recuperated one (layout 8), and they are depicted in Figure 5.

The increasing complexity of the cycles is obviously translated into a greater complexity in terms of the number and type of components and the costs. Table 1 reports the number of heat exchangers that each layout needs to operate. The heat exchanger is one of the most important and critical components of this type of plant and the most impactful component in terms of weight, volume and cost. The number of heat exchangers

therefore becomes one of the factors that have to be analyzed coupled with the energetic and exergetic performance parameters to identify the most suitable layout configuration.

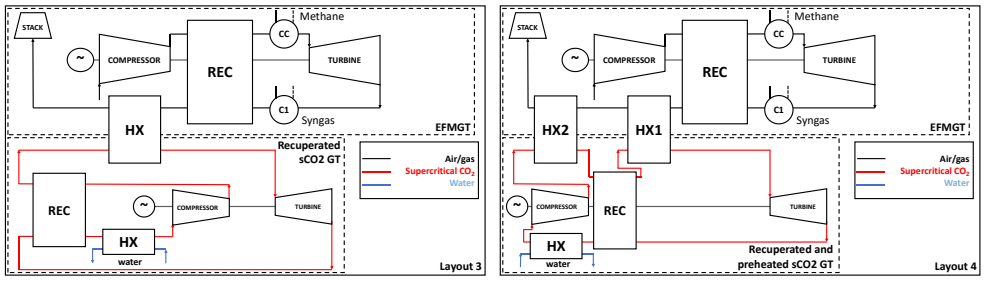

Figure 3. EFMGT plus recuperated sCO_2 GT (**left**, layout 3); EFMGT plus recuperated and preheated sCO_2 GT (**right**, layout 4).

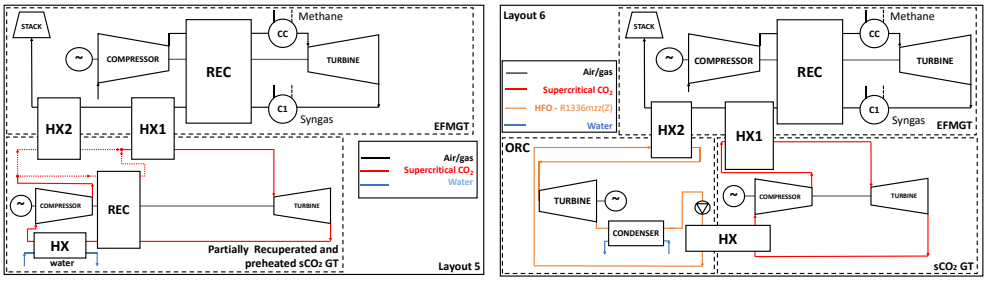

Figure 4. EFMGT plus partially recuperated and preheated sCO_2 GT (**left**, layout 5); EFMGT plus simple sCO_2 GT and simple ORC (**right**, layout 6).

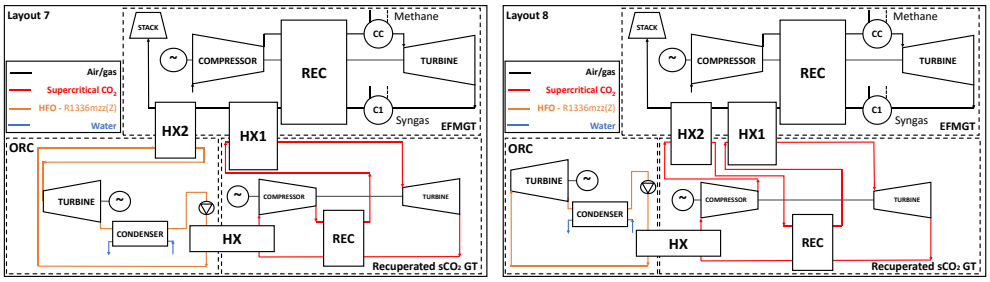

Figure 5. EFMGT plus recuperated sCO_2 GT +ORC (**left**, layout 7); EFMGT plus preheated and recuperated sCO_2 GT + ORC (**right**, layout 8).

Table 1. Layouts and components.

Layout	Brief Description	Heat Exchangers
0	EFMGT	1
1	EFMGT + ORC	4
2	EFMGT+ sCO_2 GT	3
3	EFMGT+ recuperated sCO_2 GT	4
4	EFMGT + preheated recuperated sCO_2 GT	5
5	EFMGT + partially preheated and rec. sCO_2 GT	5
6	EFMGT + sCO_2 GT + ORC	5
7	EFMGT + recuperated sCO_2 GT + ORC	6
8	EFMGT + preheated and recuperated sCO_2 GT + ORC	6

3. Hybrid Energy System Modeling

The thermodynamic analysis of the hybrid energy system is carried out through the use of the commercial software Thermoflex, provided by Thermoflow Inc. (Southborough, MA, USA) [34]. This software allows for 0D steady-state analysis based on mass and

energy balancing, considering also maps, equations and corrective factors to simulate the off-design conditions. Thermoflex enables the REFPROP—NIST property function for the gas stream to be used as required [35], which has great importance to correctly simulate the physical properties of CO_2 in supercritical conditions, especially close to the critical point [36,37]. In fact, the use of the REFPROP database, which is based on the Span–Wagner Equation of State [38], seems to be one of the most accurate approaches to simulate indirect or direct fired supercritical CO_2 Brayton cycles [39].

The dual-fuel externally fired micro gas turbine is modeled starting from a previous validated numerical model of a commercial MGT, model Turbec T100, actually provided by Ansaldo Energia as AE T100 [40]. The compressor and turbine are modeled using characteristic maps taken from the literature [41] and already used in numerical–experimental comparisons [42]. The internal combustion chamber and the heat exchanger efficiencies are also considered, as well as the pressure and thermal losses of each component.

In the absence of experimental data, it is important to highlight that numerical models built in Thermoflex have been validated for micro gas turbines derived from AE T100 [43,44], as well as for sCO_2 gas turbines [45].

The simulations are carried out considering some constraints. For the sake of simplicity, the turbine inlet temperature is fixed at 1200 K, according to the design value reported by the manufacturer, as shown in [42,43]. Indeed, radial turbines of small-scale gas turbines cannot operate with the higher temperatures typical of larger plants. With this constraint, the thermodynamic model calculates the fuel mass flow to reach this temperature level.

The maximum temperature of the exhaust gases at the inlet of the recuperator is fixed at 1173 K, considering the state of the art of high-temperature heat exchangers for externally fired gas turbines and the advantages of ceramic HTHX technology [6]. Table 2 reports the design parameters of the EFMGT.

Table 2. EFMGT's main characteristic data.

Description	Value
Compressor and turbine performance	Maps
Combustor efficiency	97%
Recuperator efficiency	90%
Turbine inlet temperature, K	1200
HX inlet temperature, K	1173

The introduction of the ORC implies the selection of the working fluid, which is one of the most critical issues related to the design of Organic Rankine Cycles. In fact, following the Montreal Protocol and its amendments [46,47], hydrochlorofluorocarbons (HCFCs) are scheduled to be phased out by 2020 in developed countries and by 2030 in developing countries, while hydrofluorocarbons (HFCs) will be reduced by 85% by 2036 in developed countries and by 80% by 2045 in developing countries.

Thus, the research focus on ORCs is currently mainly aimed at the individuation of novel working fluids. Hydrofluorolefins (HFOs) and hydrochlorofluoroolefins (HCFOs) can represent promising alternatives due to their very low global warming potential (GWP) and ozone depletion potential (ODP). The HCFOs R1233d(E) and R1224yd(Z) can be considered good alternatives to R245fa, one of the main used organic working fluids in existing ORC plants, because of their similar thermophysical properties with a significantly lower GWP [48–51]. HFOs such as R1336mzz(Z) can be considered for the same reasons [48–50,52,53].

The use of R1336mzz(Z) was experimentally investigated as a low-GWP working fluid in an ORC in the case of heat source temperatures between 140 °C and 160 °C and heat sink temperatures between 25 °C and 40 °C in [52]. In that paper, the authors stated that similar values of the overall expander–generator efficiency are obtained by comparing the two working fluids, and the electrical efficiency obtained with the HFO-1336mzzz-Z is higher than the value obtained with the HFC-245fa. For these reasons, an HFO,

cis-1,1,1,4,4,4-hexaflouro-2-butene R1336mzz(Z), is chosen as the working fluid of the ORC plant because of its low values of ODP and GWP, its low toxicity and flammability, and its behavior [42,52]. On the other hand, the temperature levels of the heat source at which this organic fluid operates are lower than the exhaust gas temperatures.

Table 3 reports the thermophysical properties of R1336mzz(Z) [52,53].

Table 3. R1336mzz(Z)'s thermophysical properties.

Description	Value
Chemical formula	$CF_3CHCHCF_3$
ODP	0
GWP 100 years	2
ASHRAE Standard 34 Safety Class [54]	A1
OEL, ppm	500
Atmospheric life time, year	0.060274
Molar weight, kg/kmol	164

A1 denotes that R1336mzz(Z) is low toxicity (A) and presents no flame propagation (1) when tested as per the standard.

The efficiency of the ORC strongly depends on the pressure ratio: the higher the pressure ratio, the higher the performance of the ORC. In this study, the pressure ratio is fixed at 5.6, considering experimental values already published in the literature [55].

The expander efficiency has been fixed at 60% considering that scroll expander isentropic efficiencies can also reach 65% in the case of R245fa as the working fluid [56] and that the mechanical isentropic efficiency is lower when R1336mzz(Z) replaces R245fa [57].

The ORC design parameters are shown in Table 4.

Table 4. ORC's main characteristic data.

Description	Value
Pump inlet pressure, bar	0.8
Turbine inlet pressure, bar	5.6
Expander efficiency,	60%
HX efficiency	90%

The identification of the design parameters of the supercritical CO_2 micro gas turbine can be achieved considering the scarcity of significant experimental data and the abundance of results of numerical simulations available in the literature.

The experiments are mainly conducted on prototypes with very low rotating component efficiencies, while the numerical/theoretical design parameters are considerably greater [27]. For these reasons, 80% can be considered a conservative and usable value for the efficiencies of the rotating components.

The modeling of the recuperator represents one of the main issues, since the significant variations in the thermodynamic properties of sCO_2 are close to the critical point: in both temperature lines, the fluid is in supercritical conditions and the different heat capacities of sCO_2 could lead to internal pinch points near to zero. This problem mainly affects the low-temperature recuperators, while at high temperatures and pressures, the difference in the specific heat is not significant [12]. This aspect can be overcome by modeling the recuperator as two or multiple heat exchangers in a series, when needed, following the solution proposed by Scaccabarozzi et al. [58]. In that specific case, the HX model does not present temperature levels that can lead to these issues.

The pressure at the inlet of the turbine is close to 200 bar, with a compressor ratio close to 2.6, since the compressor inlet pressure is fixed at 75 bar. Table 5 reports the sCO_2 GT design parameters.

Table 5. sCO_2 GT's main characteristic data.

Description	Value
Compressor p. efficiency	80%
Turbine p. efficiency	80%
Compressor inlet pressure, bar	75
Turbine inlet pressure, bar	200
HX efficiency	90%

The sizing of the hybrid energy grid follows some steps: First of all, the input thermal power has been defined. By fixing this constraint, the distribution between biomass and methane is calculated considering the limits of the turbine inlet combustor (1200 K) and that methane has to be considered a boost to obtain that value. In addition, the temperature of the cold source has to be fixed. Once the hot and cold sources are fixed, a parametrical analysis is carried out in order to identify the working fluids' mass flow able to guarantee the best performance levels.

The simulations must consider a further constraint: the carbon dioxide temperature at the compressor inlet has to be greater than its critical temperature and as close as possible to that value. The ORC details have to be chosen taking into account this aspect.

Finally, the gasifier has been modeled using a zero-dimensional approach. The model, which is embedded in Thermoflex, uses the reaction reported in (1), achieving thermochemical equilibrium between the species involved in this reaction.

$$CH_xO_yN_z + wH_2O + m(O_2 + 3.76\ N_2) \rightarrow n_{H_2}H_2 + n_{CO}CO + n_{H_2O}H_2O + n_{CH_4}CH_4 + \left(\frac{z}{2} + 3.76\ m\right)N_2 \quad (1)$$

Further details on the gasification system can be found in [27]. A key parameter in defining syngas quality and composition is the Equivalence Ratio (Equation (2)):

$$ER = \frac{\dot{m}_{air}}{\dot{m}_{biomass}} \Bigg/ \left(\frac{\dot{m}_{air}}{\dot{m}_{biomass}}\right)_{stoich} \quad (2)$$

Its value should be neither too low (<0.2) due to technological issues nor too high (>0.4), which can lead to combustion rather than gasification. Therefore, the Equivalence Ratio has been set at 0.30, an optimal value as shown in [59]. Consequently, the actual air/fuel ratio has been fixed at 1.96.

The composition of the solid fuel is listed in Table 6, while the syngas composition and characteristics are depicted in Table 7.

Table 6. Solid fuel (organic fraction of municipal solid wastes) analysis.

Description	Value	
Weight percent of ash	14.18	%
Weight percent of moisture	20	%
Weight percent of carbon	34.84	%
Weight percent of hydrogen	3.93	%
Weight percent of oxygen	24.45	%
Weight percent of nitrogen	1.46	%
Weight percent of sulfur	1.14	%
LHV	12,483	kJ/kg
HHV	13,829	kJ/kg

Table 7. Syngas composition and characteristics.

Description	Value		
Hydrogen	H_2	14.81	%
Water vapor	H_2O	12.78	%
Nitrogen	N_2	46.15	%
Carbon monoxide	CO	14.82	%
Carbon dioxide	CO_2	10.58	%
Methane	CH_4	0.0004	%
Hydrogen sulfide	H_2S	0.3027	%
Carbonyl sulfide	COS	0.0097	%
Argon	Ar	0.5504	%
LHV		3221.7	kJ/kg
HHV		3718	kJ/kg

4. Energetic and Exergetic Performance Analysis of the Hybrid Energy Systems

The electric efficiency of the hybrid energy system (HES) is defined as the ratio between the sum of net powers of each component and the primary thermal power in the input:

$$\eta_{hes} = \frac{P_{EFMGT} + P_{sCO2\ GT} + P_{ORC}}{\dot{Q}_{bio} + \dot{Q}_{CH4}} \tag{3}$$

The net power is defined as the difference between the power provided by the turbine and the value absorbed by the compressors or pumps. These values also consider the presence of the generator, with the generator efficiency fixed, for simplicity, at 94%. In addition, P_{EFMGT} is calculated considering both fuel compressors' (natural gas and syngas) power consumption: the nominal power of the gaseous fuel compressor is 3 kW [35]. The thermal power in the input is evaluated considering the contribution of methane ($\dot{Q}_{CH4}$) and the thermal power of the solid biomass in the input to the gasification system ($\dot{Q}_{bio}$). The gasification efficiency is close to 72%.

Another performance parameter of interest regards the net efficiency of the hybrid energy system calculated without considering the presence of the gasification system, thus neglecting the losses related to the gasification process and directly considering the thermal power of the syngas fuel at the fuel compressor inlet ($\dot{Q}_{syngas}$). This hybrid energy system' (HES) net efficiency is defined as follows:

$$\eta_{hes\_net} = \frac{P_{EFMGT} + P_{sCO2\ GT} + P_{ORC}}{\dot{Q}_{syngas} + \dot{Q}_{CH4}} \tag{4}$$

The waste heat recovery efficiency η_{WHR} is defined in Equation (5) and is equal to the ratio between the power obtained by the bottoming cycles and the total amount of available thermal power at the exhaust. For the sake of simplicity, $\Delta H_{HX_{MGT}}$ is the difference between the enthalpy of exhaust gases at the inlet of the heat exchanger and at the stack, with the stack temperature fixed at 373 K. This fixed value is chosen to allow for the comparison between waste heat recovery solutions that can lead to different exhaust temperatures, considering the maximum available thermal power.

$$\eta_{WHR} = \frac{P_{sCO2\ GT} + P_{ORC}}{\dot{m}_{gas} \times \Delta H_{HX_{MGT}}} \tag{5}$$

The global electrical efficiency of each component can be obtained once we have defined the thermal power in the input of each thermal cycle (Equations (3)–(5)).

$$\eta_{EFMGT} = \frac{P_{EFMGT}}{\dot{Q}_{bio} + \dot{Q}_{CH4}} \tag{6}$$

$$\eta_{sCO2GT} = \frac{P_{sCO2\ GT}}{\dot{m}_{gas} \times \Delta H_{HX_{MGT}}} \tag{7}$$

$$\eta_{ORC} = \frac{P_{ORC}}{\dot{m}_{sCO2} \times \Delta H_{HX_{sCO2GT}}} \quad (8)$$

The exergy in the input to the waste heat recovery system is the exergy transferred to the supercritical carbon dioxide from the exhausts of the EFMGT and is equal to $\Delta\xi_{HX} = \dot{m}_{gas} \times (\Delta H_{HX_{MGT}} - T_0 \times \Delta s_{HX_{MGT}})$, considering the ambient temperature as the reference condition (T_0 = 293.5 K). The exergetic efficiency of waste heat recovery is reported in Equation (9):

$$\eta_{ex_{WHR}} = \frac{P_{sCO2\ GT} + P_{ORC}}{\Delta\xi_{HX}} \quad (9)$$

5. Results

The best layout can be identified through a comparison of both the net power and global efficiency of the eight hybrid layouts, when compared with the reference case (layout 0—dual-fuel EFMGT), also considering the exergetic efficiency. The comparison has been performed in identical conditions in terms of the turbine inlet temperature (1200 K) and heat exchanger inlet temperature (1173 K) of the EFMGT and in ambient conditions. The simulations have been carried out considering identical values of heat exchanger efficiencies and losses. Solid biomass availability has been calculated considering approximately 100 kg/h, a value estimated based on the waste production of a community of around 1000 individuals. For the organic fraction of urban solid waste, whose composition is listed in Table 6, this corresponds to about 0.078 kg/s of syngas fuel.

For each layout, the mass flow of the WHR working fluid, which gives the best power level, is identified through a parametric analysis. The resulting values are reported in Figure 6.

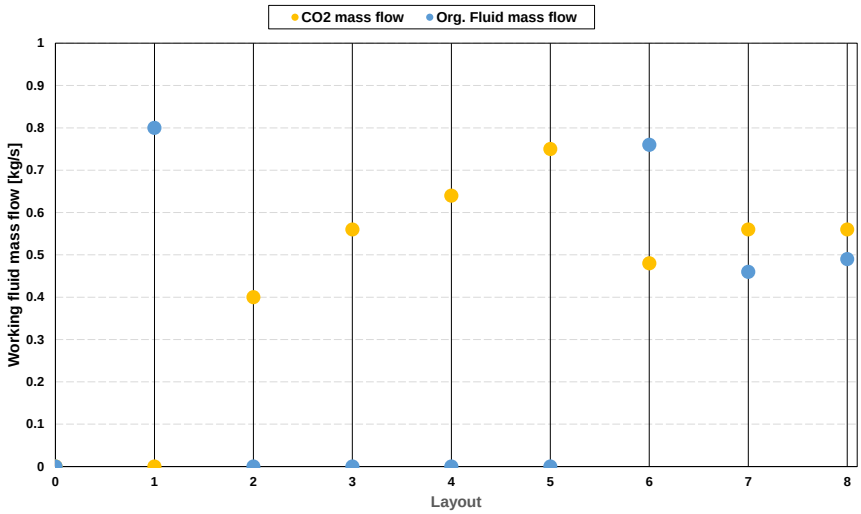

Figure 6. Working fluid mass flow of WHR energy system.

Regarding the HFO mass flow, layout 1 features a regenerative ORC as the bottoming system, whereas the ORCs embedded in layouts 6, 7 and 8 follow a simple Rankine cycle, without the internal recuperator. In the first case, the organic fluid mass flow is calculated to maximize the new power. In the other cases, the mass flow is evaluated both to optimize the net power and to allow the upper cycle to operate with a compressor inlet temperature close to or greater than the CO_2 critical temperature.

Regarding the sCO_2 mass flow, the increasing complexity of the layout leads to a greater value of the optimal mass flow.

The performance of the proposed plant arrangements in terms of electric powers and efficiencies is depicted in Figures 7 and 8, respectively. The first column of Figure 7 shows (in blue) that the EFMGT is barely capable of delivering about 80 kW. The dual-fuel

externally fired configuration allows us to limit fuel compressor power consumption, which is a severe constraint for the syngas-fueled micro gas turbines, as shown in [21]. In addition, the net power can be enhanced up to 98 kW if a WHR (SCBC, in orange, or ORC, in gray) is coupled with the dual-fuel EFMGT and up to 103 kW when both WHR systems are adopted in a cascade system. The introduction of a WHR system leads to an increase of 16–24% in the available net power, depending on the chosen layout, while the integration of both WHR systems can lead to an increase of about 29% with respect to the reference case. For all cases, the power output of the gas turbine is almost the same, with slight differences related to the back pressure induced by the number of heat exchangers at the turbine exit.

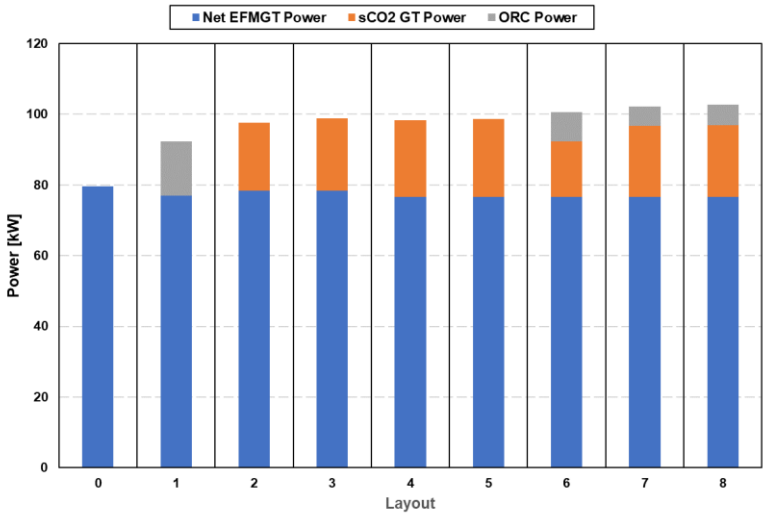

Figure 7. Hybrid energy system and WHR net power levels.

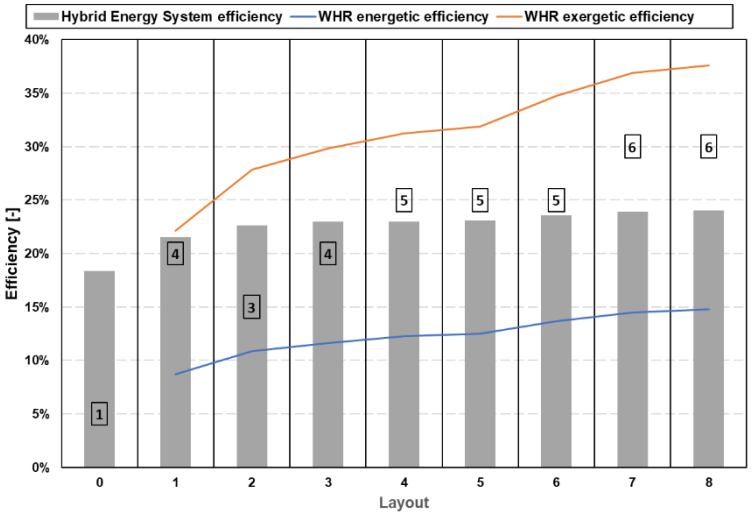

Figure 8. Hybrid energy system and WHR efficiencies and number of heat exchangers.

The chart in Figure 8 shows the plant's efficiency, as defined by Equation (3), with gray bars, the waste heat recovery efficiency with a blue line and the waste heat recovery exergy efficiency with an orange line; the WHR efficiency and the WHR exergy efficiency have been defined as in Equations (5) and (9), respectively. The number enclosed within the rectangle is a complexity index of the layout in terms of the number of required heat exchangers. The plant's efficiency for the EFMGT is 18.4% and is the lowest of all of the proposed layouts; when a single WHR system is used, the efficiency reaches 23%, while using both sCO_2 and ORC-bottomed plants, the efficiency achieves its maximum value of 24%. The WHR energetic and exergetic efficiencies increase with the increase in layout

complexity. The three layouts with both WHR systems in cascade present the highest performance, almost 15% and 37% of the energy and exergy WHR efficiency.

A further evaluation can be conducted considering the thermal power which is available to the EFMGT, neglecting the losses related to the gasification system. In this way, the thermal power in the input is the sum of the contributions from both syngas and methane. This allows for the evaluation of the net efficiency of the hybrid energy system (Equation (4)) compared to the efficiency of the EFMGT. The resulting energetic parameters are shown in Figure 9: the continuous lines refer to the net efficiency, without considering the presence of the gasifier, while the dashed–dotted lines represent the overall efficiency of the HES. It is clear that the overall system's efficiency is affected by the efficiency of the gasifier, while the efficiency of the HES alone results in being greater than 30% for layouts 5, 6, 7 and 8.

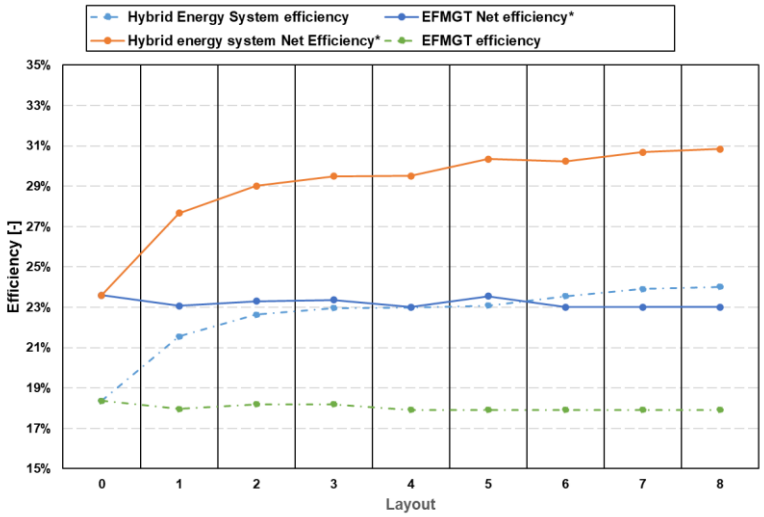

Figure 9. Hybrid energy system efficiencies ((*) the gasification system losses are neglected).

The emission levels of carbon dioxide are strictly connected to the use of methane as a secondary fuel and do not significantly vary with changes in WHR layouts. In addition, the organic fraction of municipal waste can be considered a renewable and carbon-neutral (or near-neutral) energy source, meaning that only a small portion of CO_2 emissions can be considered GHG emissions. Figure 10 shows the emissions of CO_2 calculated in kilograms for MWh. Considering the contribution of the OFSMW, more than 80% of the CO_2 emissions are neutral.

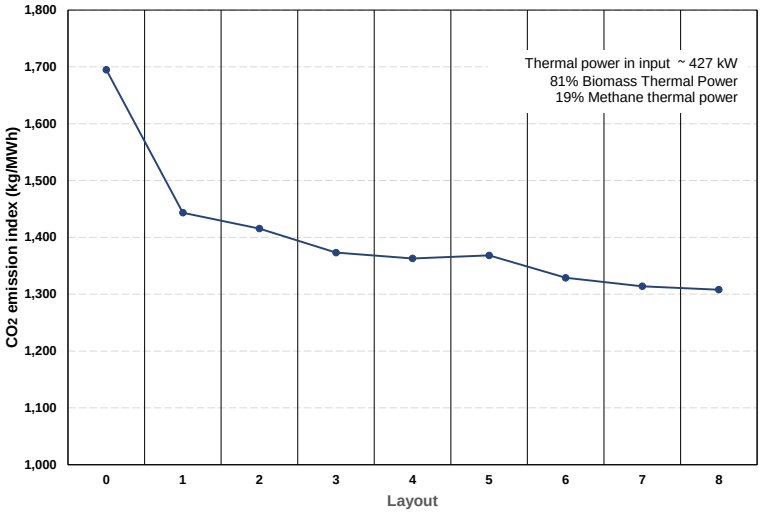

Figure 10. CO_2 emission index by varying HES layout.

The results have highlighted that the cascade layouts enhance the overall performance levels in terms of both energetic and exergetic efficiency. At the same time, this choice requires greater complexity and, consequently, higher costs. The number of heat exchangers is indicative as the HX represents the heaviest, bulkiest and most expensive component.

6. Conclusions

A small-scale hybrid energy system, which is based on an externally fired gas turbine, ORC and sCO_2 gas turbine, has been defined in order to study the opportunities related to the use of a syngas derived from the organic fraction of municipal waste. A preliminary parametric analysis has been carried out to identify the optimal working fluid mass flows when the quantity of the organic fraction of municipal waste is given and the temperature constraints have been fixed. In this study, the efficiencies and thermal/pressure losses of each component have been considered.

A performance analysis in terms of net power, thermal efficiency and exergetic efficiency has been carried out for eight different hybrid energy system layouts to obtain the best compromise between higher performance levels and enhanced complexity.

The results of the simulations highlight that the dual-fuel configuration of the EFMGT expects to attain about 80 kW with a thermal efficiency of 18.4%, considering all of the losses, including those related to the gasification system, while the thermal efficiency of the EFMGT alone is equal to 23.6%. The introduction of a WHR system leads to an increase in both the net power and efficiencies. The layout with the ORC increases the efficiency to 21.6%, with a WHR exergetic efficiency of about 22%. The sCO_2 gas turbine-based layouts improve performance. The cascade layouts, in which both the sCO_2 gas turbine and ORC are present in a series, provide an increase of about 27–29% in the net power with respect to the reference case, reaching a thermal net efficiency of 24% (30.8% neglecting the contribution of the gasification system) in the best-case scenario (layout 8). Also, considering the complexity of the hybrid system in terms of the number of heat exchangers, the sixth layout seems to be the best compromise.

Author Contributions: Conceptualization, F.R. and P.M.; methodology, F.R.; writing—original draft, F.R.; writing—review and editing, F.R. and P.M. All authors have read and agreed to the published version of the manuscript.

Funding: This study received no external funding.

Data Availability Statement: Data are contained within the article.

Conflicts of Interest: The authors declare no conflicts of interest.

Abbreviations

Bio	Biomass
EFMGT	Externally fired micro gas turbine
ER	Equivalence Ratio
GT	Gas turbine
GWP	Global warming potential
HCFO	Hydrochlorofluoroolefin
HES	Hybrid energy system
HFC	hydrofluorocarbon
HFO	Hydrofluorolefin
HHV	Higher heating value
HTHX	High-temperature heat exchanger
HX	Heat exchanger
LHV	Low heating value
MGT	Micro gas turbine
ODP	Ozone depletion potential
OEL	Occupational exposure limit

ORC	Organic Rankine Cycle
OFMW	Organic fraction of municipal waste
P	Power
REC	Recuperator
sCO_2	Supercritical CO_2
SCBC	Supercritical CO_2 Brayton cycle
TIP	Turbine inlet pressure
TIT	Turbine inlet temperature
TOP	Turbine outlet pressure
TOT	Turbine outlet temperature
WHR	Waste heat recovery
Subscripts	
El	Electrical
Greek	
η	Efficiency
ξ	Exergy

References

1. Klass, D.L. *Biomass for Renewable Energy, Fuels, and Chemicals*; Elsevier: Amsterdam, The Netherlands, 1998.
2. Perea-Moreno, M.-A.; Samerón-Manzano, E.; Perea-Moreno, A.-J. Biomass as Renewable Energy: Worldwide Research Trends. *Sustainability* **2019**, *11*, 863. [CrossRef]
3. Wichtmann, W.; Wichmann, S. Environmental, Social and Economic Aspects of a Sustainable Biomass Production. *J. Sustain. Energy Environ. Spec. Issue* **2011**, *77*, 77–81.
4. IEA. Outlook for Biogas and Biomethane: Prospects for Organic Growth, IEA, Paris; Licence: CC BY 4.0. 2020. Available online: https://www.iea.org/reports/outlook-for-biogas-and-biomethane-prospects-for-organic-growth (accessed on 10 April 2024).
5. Molino, A.; Chianese, S.; Musmarra, D. Biomass gasification technology: The state of the art overview. *J. Energy Chem.* **2016**, *25*, 10–25. [CrossRef]
6. Al-attab, K.A.; Zainal, Z.A. Externally fired gas turbine technology: A review. *Appl. Energy* **2015**, *138*, 474–487. [CrossRef]
7. Baina, F.; Malmquist, A.; Alejo, L.; Palm, B.; Fransson, T.H. Analysis of a high-temperature heat exchanger for an externally-fired micro gas turbine. *Appl. Therm. Eng.* **2015**, *75*, 410–420. [CrossRef]
8. de Mello, P.E.B.; Monteiro, D.B. Thermodynamic study of an EFGT (externally fired gas turbine) cycle with one detailed model for the ceramic heat exchanger. *Energy* **2012**, *45*, 497–502. [CrossRef]
9. Campo, P.; Benitez, T.; Lee, U.; Chung, J.N. Modeling of a biomass high temperature steam gasifier integrated with assisted solar energy and a micro gas turbine. *Energy Convers. Manag.* **2015**, *93*, 72–83. [CrossRef]
10. Datta, A.; Ganguly, R.; Sarkar, L. Energy and exergy analyses of an externally fired gas turbine (EFGT) cycle integrated with biomass gasifier for distributed power generation. *Energy* **2010**, *35*, 341–350. [CrossRef]
11. Basrawi, M.F.B.; Yamada, T.; Nakashini, K.; Katsumata, H. Analysis of the performances of biogas-fuelled micro gas turbine cogeneration systems (mGT-CGSS) in middle- and small-scale sewage treatment plants: Comparison of performances and optimization of mGTs with various electrical power outputs. *Energy* **2012**, *38*, 291–304. [CrossRef]
12. Reale, F.; Sannino, R. Numerical Modeling of Energy Systems Based on Micro Gas Turbine: A Review. *Energies* **2022**, *15*, 900. [CrossRef]
13. Traverso, A.; Massardo, A.F.; Scarpellini, R. Externally Fired micro-Gas Turbine: Modelling and experimental performance. *Appl. Therm. Eng.* **2006**, *26*, 1935–1941. [CrossRef]
14. Pantaleo, A.M.; Camporeale, S.M.; Shah, N. Thermo-economic assessment of externally fired micro-gas turbine fired by natural gas and biomass: Applications in Italy. *Energy Convers. Manag.* **2013**, *75*, 202–213. [CrossRef]
15. Riccio, G.; Chiaramonti, D. Design and simulation of a small polygeneration plant cofiring biomass and natural gas in a dual combustion micro gas turbine (BIO_MGT). *Biomass Bioenergy* **2009**, *33*, 1520–1531. [CrossRef]
16. Lecompte, S.; Huisseune, H.; van den Broek, M.; Vanslambrouck, B.; De Paepe, M. Review of organic Rankine cycle (ORC) architectures for waste heat recovery. *Renew. Sustain. Energy Rev.* **2015**, *47*, 448–461. [CrossRef]
17. Invernizzi, C.; Iora, P.; Silva, P. Bottoming micro-Rankine cycles for micro-gas turbines. *Appl. Therm. Eng.* **2007**, *27*, 100–110. [CrossRef]
18. Mago, P.J.; Chamra, L.M.; Srinivasan, K.; Somayaji, C. An examination of regenerative organic Rankine cycles using dry fluids. *Appl. Therm. Eng.* **2008**, *28*, 998–1007. [CrossRef]
19. Bonolo de Campos, G.; Bringhenti, C.; Traverso, A.; Tomita, J.T. A Review on Combining Micro Gas Turbines with Organic Rankine Cycles. In Proceedings of the E3S Web of Conference Volume 113, Savona, Italy, 4–6 September 2019. [CrossRef]
20. Javanshir, A.; Sarunac, N.; Razzaghpanah, Z. Thermodynamic Analysis of ORC and Its Application for Waste Heat Recovery. *Sustainability* **2017**, *9*, 1974. [CrossRef]

21. Reale, F.; Sannino, R.; Calabria, R.; Massoli, P. Numerical study of a small-scale micro gas turbine-ORC power plant integrated with biomass gasifier. In Proceedings of the ASME Turbo Expo 2020, Online, 21–25 September 2020. Paper No: GT2020-15401. [CrossRef]
22. Wang, Z.; Jiang, Y.; Han, F.; Yu, S.; Li, W.; Ji, Y.; Cai, W. A thermodynamic configuration method of combined supercritical CO_2 power system for marine engine waste heat recovery based on recuperative effects. *Appl. Therm. Eng.* **2022**, *200*, 117645. [CrossRef]
23. Marchionni, M.; Bianchi, G.; Tassou, S.A. Review of supercritical carbon dioxide (sCO_2) technologies for high-grade waste heat to power conversion. *SN Appl. Sci.* **2020**, *2*, 611. [CrossRef]
24. Zendehboudi, A. Energy, exergy, and exergoeconomic analyses of an air source transcritical CO_2 heat pump for simultaneous domestic hot water and space heating. *Energy* **2024**, *290*, 130295. [CrossRef]
25. Ahn, Y.; Bae, S.J.; Kim, M.; Cho, S.K.; Baik, S.; Lee, J.I.; Cha, J.E. Review of supercritical CO_2 power cycle technology and current status of research and development. *Nucl. Eng. Technol.* **2015**, *47*, 647–661. [CrossRef]
26. Crespi, F.; Gavagnin, G.; Sanchez, D.; Martinez, G.S. Supercritical carbon dioxide cycles for power generation: A review. *Appl. Energy* **2017**, *195*, 152–183. [CrossRef]
27. Martin, T.; White, M.T.; Bianchi, G.; Chai, L.; Tassou, S.A.; Sayma, A.I. Review of supercritical CO_2 technologies and systems for power generation. *Appl. Therm. Eng.* **2021**, *185*, 1164447. [CrossRef]
28. Arena, U.; Di Gregorio, F.; Santonastasi, M. A techno-economic comparison between two design configurations for a small scale, biomass-to-energy gasification based system. *J. Chem. Eng.* **2010**, *162*, 580–590. [CrossRef]
29. Tavallaei, M.; Farzaneh-Gord, M.; Moghadam, A.J. 4E analysis and thermodynamic optimization of flaring associated gas recovery using external firing recuperative gas turbine. *Energy Convers. Manag.* **2022**, *266*, 115836. [CrossRef]
30. Ancona, M.A.; Bianchi, M.; Branchini, L.; De Pascale, A.; Melino, F.; Peretto, A.; Torricelli, N. Systematic Comparison of ORC and s-CO2 Combined Heat and Power Plants for Energy Harvesting in Industrial Gas Turbines. *Energies* **2021**, *14*, 3402. [CrossRef]
31. Weiland, N.T.; Lance, B.W.; Pidaparti, S.R. sCO_2 Power Cycle Component Cost Correlations from DOE Data Spanning Multiple Scales and Applications. In Proceedings of the ASME Turbo Expo 2019, Phoenix, AZ, USA, 17–21 June 2019. [CrossRef]
32. Astolfi, M.; Romano, M.C.; Bombarda, P.; Macchi, E. Binary ORC (Organic Rankine Cycles) Power Plants for the Exploitation of Medium–Low Temperature Geothermal Sources—Part B: Techno-Economic Optimization. *Energy* **2014**, *66*, 435–446. [CrossRef]
33. Costa, M.; Massarotti, N.; Cappuccio, G.; Chang, C.T.; Shiue, A.; Lin, C.J.; Wang, Y.T. Modeling of Syngas Production from Biomass Energy Resources Available in Taiwan. *Chem. Eng. Trans.* **2014**, *37*, 343–348. [CrossRef]
34. Thermoflow Thermoflex v. 31. Available online: www.thermoflow.com (accessed on 25 May 2024).
35. Lemmon, E.W.; Bell, I.H.; Huber, M.L.; McLinden, M.O. *NIST Standard Reference Database 23: Reference Fluid Thermodynamic and Transport Properties-REFPROP, Version 10.0, National Institute of Standards and Technology*; Standard Reference Data Program: Gaithersburg, MD, USA, 2018.
36. White, C.W.; Weiland, N.T. Evaluation of Property Methods for Modeling Direct-Supercritical CO_2 Power Cycles. *J. Eng. Gas Turbines Power* **2018**, *140*, 011701. [CrossRef]
37. Zhao, Q.; Mecheri, M.; Neveux, T.; Privat, R.; Jaubert, J.-N. Thermodynamic Model Investigation for Supercritical CO_2 Brayton Cycle for Coal-Fired Power Plant Application. In Proceedings of the Fifth International Supercritical CO_2 Power Cycles Symposium 2016, San Antonio, TX, USA, 29–31 March 2016. Paper No. 93.
38. Span, R.; Wagner, W. A new equation of state for carbon dioxide covering the fluid region from the triple-point temperature to 1100 K at pressures up to 800 MPa. *J. Phys. Chem. Ref. Data* **1996**, *25*, 1509–1558. [CrossRef]
39. Reale, F. The Allam Cycle: A Review of Numerical Modeling Approaches. *Energies* **2023**, *16*, 7678. [CrossRef]
40. Ansaldo Energia AE-T100 Natural Gas Micro Turbine. Available online: https://www.ansaldoenergia.com/PublishingImages/Microturbines/AE-T100NG.pdf (accessed on 25 May 2024).
41. Caresana, F.; Pelagalli, L.; Comodi, G.; Renzi, M. Microturbogas cogeneration systems for distributed generation: Effects of ambient temperature on global performance and component's behavior. *Appl. Energy* **2014**, *124*, 17–27. [CrossRef]
42. di Gaeta, A.; Reale, F.; Chiariello, F.; Massoli, P. A dynamic model of a 100 kW micro gas turbine fuelled with natural gas and hydrogen blends and its application in a hybrid energy grid. *Energy* **2017**, *129*, 299–320. [CrossRef]
43. Reale, F.; Sannino, R. Water and steam injection in micro gas turbine supplied by hydrogen enriched fuels: Numerical investigation and performance analysis. *Int. J. Hydrogen Energy* **2021**, *46*, 24366–24381. [CrossRef]
44. Bonasio, V.; Ravelli, S. Performance Analysis of an Ammonia-Fueled Micro Gas Turbine. *Energies* **2022**, *15*, 3874. [CrossRef]
45. Reale, F.; Calabria, R.; Massoli, P. Performance Analysis of WHR Systems for Marine Applications Based on sCO_2 Gas Turbine and ORC. *Energies* **2023**, *16*, 4320. [CrossRef]
46. Montreal Protocol, UN Environment Programme. Available online: https://www.unep.org/ozonaction/who-we-are/about-montreal-protocol (accessed on 27 April 2022).
47. Montreal Protocol on Substances that deplete the Ozone layer, Australian Government. Available online: https://www.awe.gov.au/environment/protection/ozone/montreal-protocol (accessed on 27 April 2022).
48. Dawo, F.; Fleischmann, J.; Kaufmann, F.; Schifflechner, C.; Eyerer, S.; Wieland, C.; Spliethoff, H. R1224yd(Z), R1233zd(E) and R1336mzz(Z) as replacements for R245fa: Experimental performance, interaction with lubricants and environmental impact. *Appl. Energy* **2021**, *288*, 116661. [CrossRef]

49. Eyerer, S.; Wieland, C.; Vandersickel, A.; Spliethoff, H. Experimental study of an ORC (Organic Rankine Cycle) and analysis of R1233zd-E as a drop-in replacement for R245fa for low temperature heat utilization. *Energy* **2016**, *103*, 660–671. [CrossRef]
50. Yang, J.; Ye, Z.; Yu, B.; Ouyang, H.; Chen, J. Simultaneous experimental comparison of low-GWP refrigerants as drop-in replacements to R245fa for Organic Rankine cycle application: R1234ze(Z), R1233zd(E), and R1336mzz(E). *Energy* **2019**, *173*, 721–731. [CrossRef]
51. Eyerer, S.; Dawo, F.; Kaindl, J.; Wieland, C.; Spliethoff, H. Experimental investigation of modern ORC working fluids R1224yd(Z) and R1233zd(E) as replacements for R245fa. *Appl. Energy* **2019**, *240*, 946–963. [CrossRef]
52. Navarro-Esbrí, J.; Molés, F.; Peris, B.; Mota-Babiloni, A.; Kontomaris, K. Experimental study of an Organic Rankine Cycle with HFO-1336mzz-Z as a low global warming potential working fluid for micro-scale low temperature applications. *Energy* **2017**, *133*, 79–89. [CrossRef]
53. Kontomaris, K.; Simoni, L.D.; Nilsson, M.; Hamacher, T.; Risla, H.N. Combined Heat and Power from Low Temperature Heat: HFO-1336mzz(Z) as a Working Fluid for Organic Rankine Cycles. In Proceedings of the International Refrigeration and Air conditioning Conference, West Lafayette, IN, USA, 11–14 July 2016.
54. *ASHRAE Standard 34-2010*; Designation and Safety Classification of Refrigerants. ASHRAE: Atlanta, GA, USA, 2010.
55. Jang, Y.; Lee, J. Comprehensive assessment of the impact of operating parameters on sub 1-kW compact ORC performance. *Energy Convers. Manag.* **2019**, *182*, 369–382. [CrossRef]
56. De Lucia, M.; Pierucci, G.; Manieri, M.; Agostini, G.; Giusti, E.; Salvestroni, M.; Taddei, F.; Cottone, F.; Fagioli, F. Experimental Characterization of Commercial Scroll Expander for Micro-Scale Solar ORC Application: Part 1. *Energies* **2024**, *17*, 2205. [CrossRef]
57. Welzl, M.; Heberle, F.; Weith, T.; Brüggemann, D. Experimental evaluation of R1336MZZ(Z) as low GWP replacement for R245FA IN A scroll expander. In Proceedings of the 5th International Seminar on ORC Power Systems, Athens, Greece, 9–11 September 2019.
58. Scaccabarozzi, R.; Gatti, M.; Martelli, E. Thermodynamic Analysis and Numerical Optimization of the NET Power Oxy-Combustion Cycle. *Appl. Energy* **2016**, *178*, 505–526. [CrossRef]
59. Caputo, C.; Cirillo, D.; Costa, M.; La Villetta, M.; Tuccillo, R.; Villani, R. Numerical analysis of a Combined Heat and Power Generation technology from residual biomasses. *J. Energy Power Eng.* **2018**, *12*, 300–321. [CrossRef]